Quadrature Radars Naturally Benefit from Unlimited Sensing

Thomas Feuillen[†,⋆]
[†]*SnT,*
University of Luxembourg
29 Avenue J.F Kennedy, L-1855 Luxembourg.
thomas.feuillen@uni.lu

Ayush Bhandari[⋆]
[⋆]*Dept. of Electrical and Electronic Engg.*
Imperial College London
SW7 2AZ, UK.
a.bhandari@imperial.ac.uk

***Abstract*—Before any processing, radar signals need to be digitized using Analog-to-Digital Converters (ADCs). Recently, the Unlimited Sensing Framework (USF), where modulo-ADCs replace classic ADCs, has been studied in radar systems to alleviate the stringent requirements on the acquisition chain when encountering high dynamic range (HDR) scenes. In USF, the recovery of a signal from its modulo measurements relies on the embedded redundant information. This redundancy often appears through oversampling or the collections of modulo measurements of the same signal using different modulo thresholds. In this paper, we leverage, using the Hilbert Transform, the structure between channels of radars equipped with quadrature or IQ coherent demodulation to design a computational system that does not require oversampling nor the multiple acquisition of the same signal. We introduce a new algorithm, namely Hilbert-Pencil of Function (Hilbert-PoF), and we show theoretically and through simulations that it achieves perfect reconstructions in this challenging setting.**

***Index Terms*—Radar, Unlimited Sensing, High Dynamic Range**

I. Introduction

The *inverse-square law* naturally limits the use of radio-frequency (RF) sensors, such as radars [1]. This law characterizes the amplitude of the received echoes from targets as decreasing according to the square of the distance from the sensor. This high variability of the targets' echoes generates received signals that, after demodulation, exhibit a High Dynamic Range (HDR). This simple fact and an *"acquire then process"* approach to radar system design [2] lead to added complexity when designing the sensors' architecture.

Directly acquiring HDR signals using conventional acquisition chains introduces quantization errors that compromise digital resolution, thereby affecting signal processing performance. The mapping from the analog to the digital domain is carried out by Analog-to-Digital Converters (ADCs). This conversion operates within a defined dynamic range and at a fixed resolution, typically specified in terms of bits. Consequently, for a given bit budget, there is a trade-off between *allocating resources to either HDR or digital resolution.* Such a trade-off

TF thanks Ahmed Murtada for the discussions and comments. TF's work is supported by FNR CORE SURF Project, ref C23/IS/18158802/SURF. The work of AB is supported by the UK Research and Innovation council's FLF Program "Sensing Beyond Barriers via Non-Linearities" (MRC Fellowship award no. MR/Y003926/1).

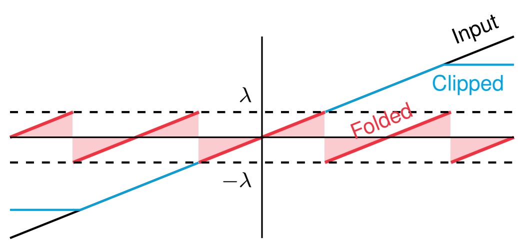

Fig. 1: Representation of the modulo acquisition $\mathscr{M}_\lambda(y(t))$ in **red** with a dynamic range $\pm\lambda$, compared to the classic ADC in **blue** with a finite dynamic range

has significant implications. Signals that exceed the dynamic range—such as high-amplitude targets—are clipped, saturating the ADC and causing a permanent loss of information, as illustrated in Fig.1 in **blue**. Conversely, variations in the signal that fall below the least significant bit of the ADC are lost in quantization noise [3].

The added complexity of the *"acquire then process"* approach in traditional RF-sensor architectures is most evident in systems that attempt to manage the dynamic range of received signals just before their acquisition. For instance, some radars dynamically adjust their sensitivity using modules like Sensitivity Time Control (STC) or Automatic Gain Control (AGC) [1]. However, for these auxiliary systems to perform as intended, strong assumptions must be made about the characteristics of the scene being measured (such as minimum and maximum ranges, velocity, etc.).

Recently, the Unlimited Sensing Framework (USF) [4] has been introduced as a new paradigm to solve the HDR acquisition challenge while maintaining digital resolution. Unlike traditional methods that decouple hardware and algorithms, the USF leverages a hardware-software co-design:

- **Hardware.** A modulo operation is introduced before the ADC in the analog domain, see Fig.1 in **red**. This ensures that the HDR signal before it is sampled lies within the acquisition range of the ADC, that is $\pm\lambda$, rendering the use of the previous strategies superfluous. Additionally, this amplitude compression provides higher digital resolution as one does not need to resolve the ambient HDR signal, rather, just quantize the range of 2λ. This new framework and its efficacy has been demonstrated in practice using prototype modulo ADCs [5], [6].

- **Algorithms.** The folded signal is algorithmically unfolded using a growing number of reconstruction methods linked with different application areas [2]–[5], [7]–[13]. These algorithms leverage the redundancy that can be found either in the time domain when over-sampling, *e.g.*, [2], [4], [5], [12], or across channels sampling the same signal [7], [8], [13], to reconstruct the HDR signal from its modulo measurements.

Motivation. These algorithms and strategies, however, only tackle the reconstruction of a single HDR signal at a time, independently of the structure, and thus redundancy, that might exist between different channels of a single sensor. Leaving this redundancy out of the reconstruction strategy is a missed opportunity that this paper seeks to remedy. In this paper, we tackle the reconstruction of HDR radar signals by leveraging the interplay between the *In-Phase* and *Quadrature* signals generated by a coherent, also called quadrature, demodulator used in Continuous Wave systems [1].

Contributions. Our contributions to this new problem of exploiting the redundancy in multi signals systems are the following: (*i*) through careful modelling, we leverage the link between the $\mathbb{I}$ and $\mathbb{Q}$ radar channels via the Hilbert transform and introduce a new algorithm *Hilbert-Pencil of Function* (Hilbert-PoF) to solve the recovery in this setting, (*ii*) we prove that this algorithm can perfectly reconstruct any HDR radar signal from its IQ modulo measurements provided that the number of combined folding instant from both modulo channels represent less than 33% of the samples of one channel, (*iii*) this is achieved without oversampling the signals or using multiple sampling of a signal with different modulo thresholds, (*iv*) we illustrate this performance through simulations and showcase a reconstruction error of -118dB.

The paper is structured as follows: Sec.II introduces the IQ radar system model, Sec.III the modulo-based acquisition model, Sec.IV presents our reconstruction strategy with its associated recovery guarantee, and finally, Sec.V showcases the simulations results before concluding in Sec.VI.

Notations. c is the speed of light, $\sqrt{-1} = \mathsf{i}$, Δ is the finite difference of order 1, S is the anti difference or cumulative sum operator, vectors (*e.g.*, $x[n] \in \mathbb{R}^N$) are represented in bold as $\boldsymbol{x}$, the Discrete Fourier Transform of a vector $\boldsymbol{x} \in \mathbb{C}^N$ is defined as $\mathscr{F}(\boldsymbol{x}, \omega) = \sum_{n=0}^{N-1} x[i] e^{-\mathrm{i}n\omega}$, with the inverse DFT $\mathscr{F}^{-1}(\cdot, N)$ defined accordingly with N being the number of samples, $\odot$ is the pointwise multiplication of vectors, $\lfloor \cdot \rfloor$ is the lower floor operator, the shifted delta $\boldsymbol{\delta}^i \in \mathbb{Z}^{N-1}$ is defined as $\delta^i[i] = 1$ and zero elsewhere. The subscripts $\cdot_{\mathbb{I}}$, $\cdot_{\mathbb{Q}}$, and $\cdot_{\mathbb{C}}$ represent, respectively, for complex signals the real (In phase) part, the imaginary (Quadrature phase) part, and the whole complex signal. $\mathrm{H}_N^M(\boldsymbol{x})$ defines the $M \times N$ Hankel matrix created from the vector $\boldsymbol{x}$. The first-order finite difference is defined as $\Delta a[k] = a[k+1] - a[k]$.

II. System Model: Radars with I/Q demodulation

We consider complex radar signals resulting from the coherent demodulation (sometimes also called quadrature demodulation or IQ demodulation) as depicted in Fig.2 ignoring for now the modulo operation $\mathscr{M}_\lambda(\cdot)$. For the sake of brevity, we will focus on a simple mono-frequency continuous wave (CW) Doppler radar in this paper. However, our approach is fully compatible with other radar systems, RF sensors, and various modulation schemes.

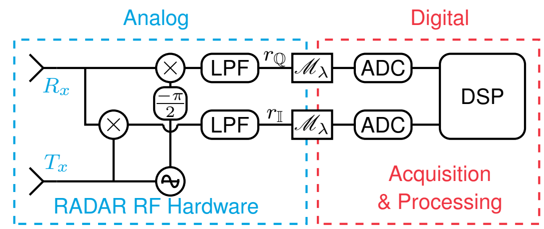

Fig. 2: IQ-based or Quadrature architecture for (FM)CW radars. The bridge between the analog and digital performed by the modulo operator $\mathscr{M}_\lambda$ thanks to the co-design approach is highlighted.

Let us consider a radar with one transmit and receive antenna transmitting at a carrier frequency at f_0. Considering a target located at a range R and approaching the radar with a radial velocity v, the received signal is

$$r(t) = \alpha \cos\left(2\pi(f_0 + \frac{2f_0 v}{\mathsf{c}})t + \phi - \frac{2R}{\mathsf{c}}\right),$$

where the shift in frequency $\frac{2f_0v}{\mathsf{c}}$ is simply the Doppler shift and α is the received power from the target. Sampling this signal directly results in an extremely demanding sampling rate requirement, as $\frac{2f_0v}{\mathsf{c}} \ll f_0$.

Coherent demodulation enables the acquisition of only the changes around the carrier, *i.e.*, the signal resulting from the Doppler effect ($f_D = \frac{2f_0v}{\mathsf{c}}$). The coherent demodulator outputs the following zero-mean signals

$$r_{\mathbb{I}}(t) = \alpha \cos(2\pi f_D t + \psi),\ r_{\mathbb{Q}}(t) = \alpha \sin(2\pi f_D t + \psi).$$

Combining these two channels, one can obtain the complex baseband signal

$$r_{\mathbb{C}}(t) = r_{\mathbb{I}}(t) + \mathsf{i} r_{\mathbb{Q}}(t) = \alpha e^{\mathsf{i}\psi} e^{\mathsf{i}2\pi f_D t}.$$

The signal's bandwidth to be acquired is now only proportional to the target's Doppler effect f_D. This model can be easily extended for a scene with K targets

$$r_{\mathbb{C}}(t) = r_{\mathbb{I}}(t) + \mathsf{i} r_{\mathbb{Q}}(t) = \sum_{k=1}^{K} \alpha_k e^{\mathsf{i}\psi_k} e^{\mathsf{i}2\pi f_{D_k} t}. \tag{1}$$

Once $r_{\mathbb{C}}(t)$ has been acquired (or recovered), the target detection process reduces to a spectral estimation problem, with all the associated conditions on the acquisition for its successful estimation.

III. Acquisition model: Unlimited Sampling

We consider the following non-linear modulo acquisition

$$z_{\mathbb{I}}[n] = \mathscr{M}_\lambda(r_{\mathbb{I}}(nT_s)),\ z_{\mathbb{Q}}[n] = \mathscr{M}_\lambda(r_{\mathbb{Q}}(nT_s)),$$

with T_s the sampling rate, and $\mathscr{M}_\lambda(y) = 2\lambda\left(\frac{y}{2\lambda} - \lfloor\frac{y+\lambda}{2\lambda}\rfloor\right)$ the modulo operator with a modulo threshold $\pm\lambda$ (see Fig.1).

We consider here identical thresholds for both channels to clearly highlight the difference with [7], see Fig.2. However, our proposed scheme is actually agnostic to the thresholds used, as will be made more explicit in the next section. Of course, in a practical setting, the measurements $\boldsymbol{z}_{\mathbb{I}}$ and $\boldsymbol{z}_{\mathbb{Q}}$ will be digitized with a finite resolution ADC. We postpone the study of the effect of quantization on our proposed system to a later publication and omit thus the quantization noise from our acquisition model.

Any modulo measurements $\boldsymbol{z} = \mathscr{M}_{\lambda}(\boldsymbol{r}) \in \mathbb{R}^N$ can be expressed as

$$\boldsymbol{z} = \mathscr{M}_{\lambda}(\boldsymbol{r}) = \boldsymbol{r} - \boldsymbol{\epsilon}, \tag{2}$$

with the residue $\boldsymbol{\epsilon} \in 2\lambda\mathbb{Z}^N$. From (2), recovering the HDR signal $\boldsymbol{r} \in \mathbb{R}^N$ amounts to estimating the residue $\boldsymbol{\epsilon}$ from $\boldsymbol{z}$.

We finish this section by introducing a rapid overview of the mechanics behind the recovery of [7], which will contextualize our reconstruction strategy using IQ radar signals. In [7], redundancy is achieved by sampling the signal twice with two different modulo thresholds λ_1, λ_2. The residues are estimated thanks to (2) by computing $\mathscr{M}_{\lambda_1}(\boldsymbol{r}) - \mathscr{M}_{\lambda_2}(\boldsymbol{r}) = \boldsymbol{\epsilon}_1 - \boldsymbol{\epsilon}_2$. The unknown HDR signal $\boldsymbol{r}$ is subtracted and only the residues remain to be estimated thanks to a relationship between λ_1 and λ_2. It is the subtraction of shared, and thus redundant, signals between $\boldsymbol{z}_{\mathbb{I}} = \mathscr{M}_{\lambda}(\boldsymbol{r}_{\mathbb{I}})$ and $\boldsymbol{z}_{\mathbb{Q}} = \mathscr{M}_{\lambda}(\boldsymbol{r}_{\mathbb{Q}})$ that we leverage our in recovery strategy.

IV. Reconstruction Strategy: Hilbert-PoF

Our reconstruction strategy follows the common scheme laid out in [4], [5], [7], which is: *(i)* leveraging the system's structure to remove the unknown HDR signals from the modulo measurements $\boldsymbol{z}_{\mathbb{I}}$, $\boldsymbol{z}_{\mathbb{Q}}$, *(ii)* estimating the residues. In the context of IQ radar systems, we carry out this first step thanks to the following relationship:

Lemma 1 (Hilbert transform for Quadrature demodulation)**.** *For received signals as defined in* (1) *sampled for a whole period at* $\frac{1}{T_s} \geq 2f_{D_{max}}$*, with* $f_{D_k} \geq 0$*, the discrete Hilbert transform* $\mathscr{H}(\cdot)$ *gives*

$$\mathscr{H}(\boldsymbol{r}_{\mathbb{Q}}) = \boldsymbol{r}_{\mathbb{I}},$$

with the Discrete Hilbert transform of a vector $\boldsymbol{x} \in \mathbb{C}^N$ *is defined as*

$$\mathscr{H}(\boldsymbol{x}) = \mathscr{F}^{-1}\left(\mathrm{i}\mathscr{F}(\boldsymbol{x}, \boldsymbol{\omega}_N) \odot sign(\boldsymbol{\omega}_N), N\right),$$

with $\omega_N = [2\pi\frac{1}{N} - \pi, \ldots, 2\pi\frac{N-1}{N} - \pi, \pi]$.

Combining Lemma 1 with the recovery strategy of [7], we can observe that

$$\boldsymbol{z}_{\mathbb{I}} - \mathscr{H}(\boldsymbol{z}_{\mathbb{Q}}) = \mathscr{H}(\boldsymbol{\epsilon}_{\mathbb{Q}}) - \boldsymbol{\epsilon}_{\mathbb{I}}. \tag{3}$$

We see in (3) that imposing the periodicity and positive (or negative) only Doppler frequency allows us to access $\boldsymbol{r}_{\mathbb{I}}$ from the modulo measurement $\boldsymbol{z}_{\mathbb{Q}}$, *i.e.*, to *leverage the redundancy across different signals*.

To estimate the residues from (3), we propose to recast the problem into a frequency estimation problem. This echoes the Fourier Prony algorithm [5], but without the need for oversampling. We do so by applying the finite difference operator to (3).

$$\boldsymbol{g} = \Delta\left(\boldsymbol{z}_{\mathbb{I}} - \mathscr{H}(\boldsymbol{z}_{\mathbb{Q}})\right) = \Delta\mathscr{H}(\boldsymbol{\epsilon}_{\mathbb{Q}}) - \Delta\boldsymbol{\epsilon}_{\mathbb{I}}. \tag{4}$$

We then notice that the residues being simple functions, their first order difference can be expressed as a sum of deltas located at their folding instants. For the $\mathbb{I}$ channel, it can be expressed as $\Delta\boldsymbol{\epsilon}_{\mathbb{I}} = \sum_{i \in \mathcal{M}_{\mathbb{I}}} \boldsymbol{\delta}^i c_{\mathbb{I}}^i$, with $c_{\mathbb{I}}^i \in 2\lambda\mathbb{Z}$ being the coefficient corresponding to the folds occurring at indexes in $\mathcal{M}_{\mathbb{I}}$. In the frequency domain, (4) becomes

$$\mathscr{F}(\boldsymbol{g}, \omega) = \mathscr{F}(\Delta\mathscr{H}(\mathsf{S}\sum_{q \in \mathcal{M}_{\mathbb{Q}}} c_{\mathbb{Q}}^q \boldsymbol{\delta}^q)) - \sum_{i \in \mathcal{M}_{\mathbb{I}}} c_{\mathbb{I}}^i e^{\mathrm{i}i\omega}. \tag{5}$$

Given the definition of the discrete Hilbert transform in Lemma 1, one can see, $\mathscr{F}(\mathscr{H}(\cdot), \omega) = \mathrm{i}sign(\omega)\mathscr{F}(\cdot, \omega)$. Thus, by addressing each part of the spectrum separately, (5) becomes

$$\boldsymbol{y}^+ = \mathscr{F}(\boldsymbol{g}, \omega \geq 0) = \mathrm{i}\sum_{q \in \mathcal{M}_{\mathbb{Q}}} c_{\mathbb{Q}}^q e^{\mathrm{i}q\omega} - \sum_{i \in \mathcal{M}_{\mathbb{I}}} c_{\mathbb{I}}^i e^{\mathrm{i}i\omega},$$
$$\boldsymbol{y}^- = \mathscr{F}(\boldsymbol{g}, \omega < 0) = -\mathrm{i}\sum_{q \in \mathcal{M}_{\mathbb{Q}}} c_{\mathbb{Q}}^q e^{\mathrm{i}q\omega} - \sum_{i \in \mathcal{M}_{\mathbb{I}}} c_{\mathbb{I}}^i e^{\mathrm{i}i\omega}.$$

On these reduced domains, the Hilbert transform manifests itself as a phase-shift $\pm\mathrm{i} = e^{\pm\mathrm{i}\frac{\pi}{2}}$ on the sum of exponential corresponding to the residue $\boldsymbol{\epsilon}_{\mathbb{Q}}$. Equation (5) is now a sum of $|\mathcal{M}_{\mathbb{C}}| = |\mathcal{M}_{\mathbb{I}} \cup \mathcal{M}_{\mathbb{Q}}|$ exponentials whose frequencies define an index, and its real part its contribution to $\boldsymbol{\epsilon}_{\mathbb{I}}$ and imaginary part to $\boldsymbol{\epsilon}_{\mathbb{Q}}$. One can notice that the frequency content remains the same on both sides of the spectrum, only the coefficients change.

We use the Generalized Pencil of Function method, also called Matrix Pencil method [14], [15] to identify the complex exponentials from the two restricted spectrums and associate them to their corresponding folds in $\Delta\boldsymbol{\epsilon}_{\mathbb{I}}$ and $\Delta\boldsymbol{\epsilon}_{\mathbb{Q}}$. We extend the classic rectangular Hankel matrices used to estimate the eigenvalues, which are then linked to frequencies, by considering both sides of the spectrum $\boldsymbol{y}^+, \boldsymbol{y}^- \in \mathbb{C}^{\frac{N}{2}}$ by leveraging their common frequency content. We concatenate the corresponding two $(\frac{N}{2} - L) \times L + 1$ Hankel matrices built from each part of the spectrum as one $2(\frac{N}{2} - L) \times L + 1$ matrix. We then set pencil parameter L as $\frac{N}{3} - 1$ to maximize the number of folds (*i.e.*, $|\mathcal{M}_{\mathbb{C}}|$) that can be recovered. This gives us the following recovery guarantee.

Recovery Guarantee Given signals $\boldsymbol{r}_{\mathbb{I}}$ and $\boldsymbol{r}_{\mathbb{Q}}$, whose structure follows Lemma 1, a sufficient condition for recovery using Hilbert-PoF, defined in Alg.1, from $\boldsymbol{z}_{\mathbb{I}}, \boldsymbol{z}_{\mathbb{Q}}$ is that the number of combined folding instants respects $|\mathcal{M}_{\mathbb{C}}| < \frac{N}{3}$.

From Alg.1, several things can be noted. First, the algorithm relies on the structure of the signal enclosed between $r_{\mathbb{I}}(t)$ and $r_{\mathbb{Q}}(t)$ and nothing else for its reconstruction. Indeed, Alg.1 is agnostic to the modulo thresholds used. Second, the reconstruction takes place at the sampling rate required for the acquisition of either $r_{\mathbb{I}}(t)$ or $r_{\mathbb{Q}}(t)$ (which is twice as high as the one for $r_{\mathbb{C}}(t)$). In this context, neither the Unlimited

Algorithm 1: Hilbert-PoF

Data: $\boldsymbol{z}_{\mathbb{I}}, \boldsymbol{z}_{\mathbb{Q}} \in \mathbb{R}^N, L = \frac{N}{3} - 1, M = \frac{N}{2}$

Result: $\boldsymbol{r}_{\mathbb{I}} = \boldsymbol{z}_{\mathbb{I}} + \hat{\boldsymbol{\epsilon}}_{\mathbb{I}}, \boldsymbol{r}_{\mathbb{Q}} = \boldsymbol{z}_{\mathbb{Q}} + \hat{\boldsymbol{\epsilon}}_{\mathbb{Q}}$

$\boldsymbol{g} = \Delta(\boldsymbol{z}_{\mathbb{I}} - \mathscr{H}(\boldsymbol{z}_{\mathbb{Q}}))$; `estimating (4)`

$\boldsymbol{y}^+ = \mathscr{F}(\boldsymbol{g}, \boldsymbol{\omega} \geq 0), \boldsymbol{y}^- = \mathscr{F}(\boldsymbol{g}, \boldsymbol{\omega} < 0)$; `DFTs`

$\boldsymbol{Y} = [\mathrm{H}_{L+1}^{M-L}(\boldsymbol{y}^+)^\top, \mathrm{H}_{L+1}^{M-L}(\boldsymbol{y}^-)^\top]^\top$; `Hankel mat*`

$\hat{\boldsymbol{\epsilon}}_{\mathbb{I}} + \mathrm{i}\hat{\boldsymbol{\epsilon}}_{\mathbb{Q}} = GPoF(\boldsymbol{Y}, L)$; `using [14]`

Sampling algorithm [4] nor the Fourier-Prony algorithm [5] would yield successful reconstructions.

V. Simulations

In this section, we compare our bespoke algorithm for IQ radar systems to other modulo-unfolding algorithms and demonstrate our recovery guarantee in a non-oversampled setting. We do so by generating a 1-periodic bandlimited analytic signal, its real and imaginary part being equivalent to $r_{\mathbb{I}}(t)$ and $r_{\mathbb{Q}}(t)$ in Fig.3. A modulo operation $\mathscr{M}_\lambda(\cdot)$ with a modulo threshold $\lambda = 2.4\text{V}$ is then applied to both channels before being sampled at the Nyquist rate with respect to one of the channels, giving $N = 100$ samples. The combined number of folding instants in both modulo channels in Fig.3 is $|\mathcal{M}_{\mathbb{C}}| = 30 < \frac{N}{3}$.

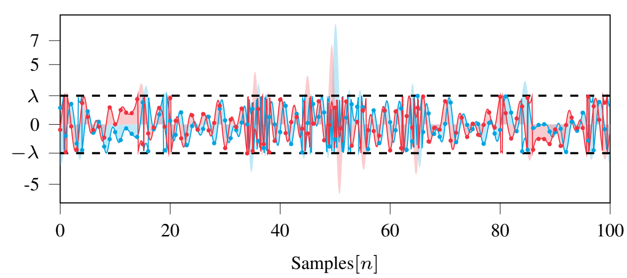

Fig. 3: The analog signals $r_{\mathbb{I}}(t)$ ( ) and $r_{\mathbb{Q}}(t)$ ( ), and their modulo equivalent $\mathscr{M}_\lambda(r_{\mathbb{I}}(t))$ ( ), $\mathscr{M}_\lambda(r_{\mathbb{Q}}(t))$ ( ), and the sampled signals $\boldsymbol{z}_{\mathbb{I}}$ ( ) and $\boldsymbol{z}_{\mathbb{Q}}$ ( ) at a rate $\frac{1}{T_s}$

To highlight the complex reconstruction setting of recovering $(\boldsymbol{r}_{\mathbb{I}}, \boldsymbol{r}_{\mathbb{Q}})$ from $(\boldsymbol{z}_{\mathbb{I}}, \boldsymbol{z}_{\mathbb{Q}})$, given the lack of oversampling, we showcase the reconstruction obtained from mono-channel algorithms. In this setting, the sampling requirement of the classic mono-channel recovery Unlimited Sampling [4] algorithm is not met. This algorithm reduces to the classic Unwrapping algorithm [16], which fails to recover the signals, Fig.4. The Fourier-Prony algorithm [5] cannot be used in this setting as it relies on oversampling to separate the residue from the signal. The same goes for techniques based on multiple thresholds (*e.g.*, [7], [8], [13]) as the thresholds used on both channels are identical. The signal corresponding to equation (4), which is central to this work, is presented in Fig.5 along with the residues $\Delta\epsilon_{\mathbb{I}}$ and $\Delta\epsilon_{\mathbb{Q}}$ to estimate. One can notice that folds of more than the modulo's dynamic range, 2λ, have to be recovered. It is from this signal that the spectral estimation is performed. Finally, Fig.6 shows the recovered signals from the modulo measurements using Alg.1. The NMSE, defined as

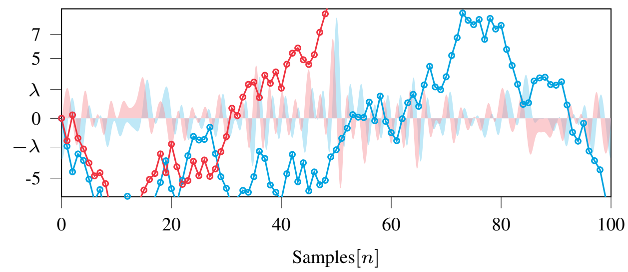

Fig. 4: The analog signals $r_{\mathbb{I}(t)}$ ( ) and $r_{\mathbb{Q}(t)}$ ( ), the reconstructed signals using the US algo [4] $\tilde{\boldsymbol{r}}_{\mathbb{I}}$ ( ) and $\tilde{\boldsymbol{r}}_{\mathbb{Q}}$ ( )

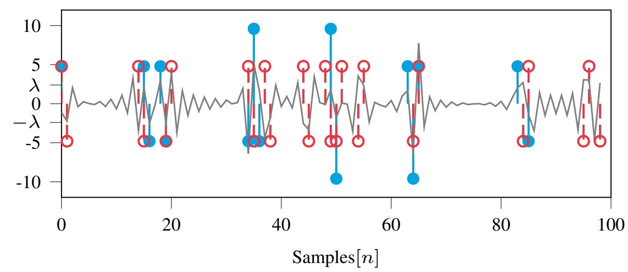

Fig. 5: Eq.(4) ( ), the residues to estimate $\Delta\boldsymbol{\epsilon}_{\mathbb{I}}$ ( ) and $\Delta\boldsymbol{\epsilon}_{\mathbb{Q}}$ ( )

$\frac{1}{2}\|\boldsymbol{r}_{\mathbb{I}} - \hat{\boldsymbol{r}}_{\mathbb{I}}\|_2^2 \|\boldsymbol{r}_{\mathbb{I}}\|_2^{-2} + \frac{1}{2}\|\boldsymbol{r}_{\mathbb{Q}} - \hat{\boldsymbol{r}}_{\mathbb{Q}}\|_2^2 \|\boldsymbol{r}_{\mathbb{Q}}\|_2^{-2}$ exceeds -118dB; the recovery is perfect.

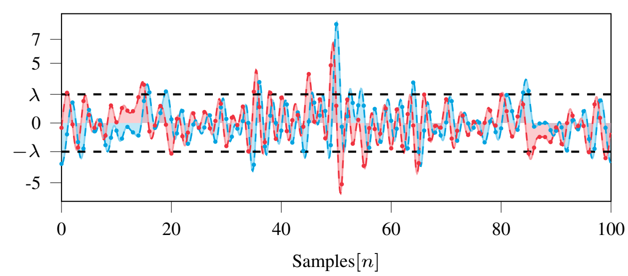

Fig. 6: The analog signals $r_{\mathbb{I}}(t)$ ( ) and $r_{\mathbb{Q}}(t)$ ( ), and the reconstruction using Alg.1 $\hat{\boldsymbol{r}}_{\mathbb{I}}$ ( ) and $\hat{\boldsymbol{r}}_{\mathbb{Q}}$ ( ), the corresponding dashed line are the sinc interpolations

VI. Conclusions and Future Work

In this paper, we demonstrated how redundancy between different signals can be leveraged in USF. We showcased this in the context of IQ, also called Quadrature, radars equipped with coherent demodulation. Our dedicated algorithm, Hilbert-PoF, thanks to one assumption on the radar scene that links the IQ channels through the Hilbert transform, can provably recover IQ signals of unknown dynamic range from their modulo measurements without any over-sampling, given a condition on the combined number of folding instants. The algorithm's accuracy was showcased using simulations and compared to the US algorithm, as other algorithms cannot operate in the considered setting. An NMSE of below -118dB was demonstrated. This work should be seen as proof of concept for applying USF to multi-channel sensors without hinging the recovery on oversampling or redundant modulo acquisitions.

REFERENCES

[1] M.I. Skolnik, *Radar Handbook, Third Edition*, Electronics electrical engineering. McGraw-Hill Education, 2008.

[2] Samuel Fernández-Menduiña, Felix Krahmer, Geert Leus, and Ayush Bhandari, "Computational array signal processing via modulo non-linearities," *IEEE Transactions on Signal Processing*, vol. 70, pp. 2168–2179, 2022.

[3] Thomas Feuillen, Bhavani Shankar MRR, and Ayush Bhandari, "Unlimited sampling radar: Life below the quantization noise," in *ICASSP 2023 - 2023 IEEE International Conference on Acoustics, Speech and Signal Processing (ICASSP)*, 2023, pp. 1–5.

[4] Ayush Bhandari, Felix Krahmer, and Ramesh Raskar, "On unlimited sampling and reconstruction," *IEEE Transactions on Signal Processing*, vol. 69, pp. 3827–3839, 2021.

[5] Ayush Bhandari, Felix Krahmer, and Thomas Poskitt, "Unlimited sampling from theory to practice: Fourier-prony recovery and prototype adc," *IEEE Transactions on Signal Processing*, vol. 70, pp. 1131–1141, 2022, arXiv:2105.05818 [cs, eess, math].

[6] Yuliang Zhu and Ayush Bhandari, "Unleashing dynamic range and resolution in unlimited sensing framework via novel hardware," , no. arXiv:2410.20193, Oct. 2024, arXiv:2410.20193 [eess].

[7] Ruiming Guo and Ayush Bhandari, "Unlimited sampling of fri signals independent of sampling rate," in *ICASSP 2023 - 2023 IEEE International Conference on Acoustics, Speech and Signal Processing (ICASSP)*, 2023, pp. 1–5.

[8] Yuliang Zhu, Ruiming Guo, Peiyu Zhang, and Ayush Bhandari, "Frequency estimation via sub-nyquist unlimited sampling," in *ICASSP 2024 - 2024 IEEE International Conference on Acoustics, Speech and Signal Processing (ICASSP)*, 2024, pp. 9636–9640.

[9] Matthias Beckmann, Ayush Bhandari, and Felix Krahmer, "The modulo radon transform: Theory, algorithms, and applications," *SIAM Journal on Imaging Sciences*, vol. 15, no. 2, pp. 455–490, 2022.

[10] Abijith Jagannath Kamath and Chandra Sekhar Seelamantula, "Neuromorphic sensing meets unlimited sampling," in *ICASSP 2024 - 2024 IEEE International Conference on Acoustics, Speech and Signal Processing (ICASSP)*, 2024, pp. 9731–9735.

[11] Thomas Feuillen, Mohammad Alaee-Kerahroodi, Ayush Bhandari, Bhavani Shankar M. R, and Björn Ottersten, "Unlimited sampling for fmcw radars: A proof of concept," in *2022 IEEE Radar Conference (RadarConf22)*, 2022, pp. 1–5.

[12] Elad Romanov and Or Ordentlich, "Above the nyquist rate, modulo folding does not hurt," *IEEE Signal Processing Letters*, vol. 26, no. 8, pp. 1167–1171, Aug. 2019.

[13] Lu GAN and Hongqing Liu, "High dynamic range sensing using multi-channel modulo samplers," in *2020 IEEE 11th Sensor Array and Multichannel Signal Processing Workshop (SAM)*, June 2020, p. 1–5.

[14] Y. Hua and T.K. Sarkar, "Generalized pencil-of-function method for extracting poles of an em system from its transient response," *IEEE Transactions on Antennas and Propagation*, vol. 37, no. 2, pp. 229–234, 1989.

[15] T.K. Sarkar and O. Pereira, "Using the matrix pencil method to estimate the parameters of a sum of complex exponentials," *IEEE Antennas and Propagation Magazine*, vol. 37, no. 1, pp. 48–55, 1995.

[16] Kazuyoshi Itoh, "Analysis of the phase unwrapping algorithm," *Appl. Opt.*, vol. 21, no. 14, pp. 2470–2470, Jul 1982.